Epitaxial mismatch strain in $YBa_2Cu_3O_{7-\delta}/PrBa_2Cu_3O_7$ superlattices

M. Varela,[1,2] D. Arias,[1,*] Z. Sefrioui,[1] C. León,[1] C. Ballesteros,[2] and J. Santamaria[1]
[1]*GFMC, Departamento de Fisica Aplicada III, Facultad de Fisica, Universidad Complutense de Madrid, Madrid 28040, Spain*
[2]*Departamento de Fisica, Universidad Carlos III de Madrid, Leganés 28911-Madrid, Spain*
(Received 18 April 2000)

The effects of epitaxial strain in ultrathin $YBa_2Cu_3O_{7-\delta}$ layers have been investigated by x-ray diffraction and transmission electron microscopy. The samples used were high quality $[YBa_2Cu_3O_{7-\delta}\,(YBCO)_N/PrBa_2Cu_3O_7\,(PBCO)_M]_{1000\,\text{Å}}$ superlattices, grown by high oxygen pressure sputtering, with N ranging between 1 and 12 unit cells and $M=5$ unit cells. Superlattice structure is refined by fitting x-ray spectra to a structural model containing disorder related parameters. Epitaxial mismatch strain and the absence of step disorder are found for YBCO layer thickness below 4 unit cells. A surprising reorganization of interatomic distances results, which seems to correlate with the decrease in the critical temperature. For larger YBCO layer thickness, stress relaxes and step disorder builds up. Transmission electron microscopy observations show the presence of *a*-axis orientated microdomains, which seem to be correlated to the release of epitaxial strain, provided in plane mismatch is smaller in this orientation.

I. INTRODUCTION

There is wide evidence on the important role played by structure on the superconducting properties of high-T_c cuprates. A large number of studies have been devoted to study the structural behavior of these complex oxides under external applied forces, such as uniaxial strains or hydrostatic pressure,[1,2] or cation substitution,[3] looking for correlations between structural rearrangements and changes in the critical temperature. The main point of interest is to find what intracell distances are relevant to the mechanism of superconductivity. Structural changes may seriously influence the superconducting properties of ultrathin epitaxial films. When reducing the layer thickness down to a small number of unit cells, lattice mismatch to the substrate may seriously affect structure, in the form of epitaxial strain. The net effect of epitaxial stress will result in a strain pattern not attainable under hydrostatic pressures or the superposition of uniaxial strains.[4] On the other hand, step disorder may cause that, although the average thickness may stay at the desired value, layer thickness fluctuations may locally break the continuity of the layer, affecting the transport properties of ultrathin layers. Strain induced structural modifications should be considered when trying to address this issue. Anyway, from this starting point, Locquet *et al.* have been able to double the critical temperature in the $La_{1.9}Sr_{0.1}CuO_4$ high-T_c superconductor using mismatch strain.[5] They show that compressive in plane epitaxial strain can generate much larger increases of T_c than those obtained by comparable hydrostatic pressures.

In presence of lattice mismatch there are two main growth modes depending whether thickness is above or below a critical value, t_c. For layer thickness below t_c there is a pseudomorphic growth of the film on the substrate, through a deformation of the crystal lattice. In this way, if the misfit between a substrate and the growing epitaxial layer is sufficiently small, the first atomic layers which are deposited will be elastically strained to match the substrate through a coherent interface, which minimizes the interface energy. This strain may not only modify in plane lattice parameters, but also may result in a lattice distortion along the out of plane direction. According to the Poisson effect, film growth on a substrate with slightly smaller (larger) in plane lattice parameters may lead to a compression (expansion) in the ab plane that can result in an expansion (contraction) in the out of plane direction.[6] On the other hand, as the layer thickness increases, the stored strain energy becomes so large at the critical thickness that misfit dislocations become energetically favorable to relax the crystal strain. When this critical thickness is exceeded, the lattice relaxes to its own lattice constants, and a new distribution of structural defects arises.

It is clear that quantitative structural investigations including disorder related parameters are essential to understand the properties of ultrathin films. X-ray diffraction (XRD) is a nondestructive widely used technique to analyze structure, which supplies structural information on the atomic scale, averaged over a length scale (structural coherence length) which may be around hundred angstroms. The extraction of quantitative information requires the fit of the diffraction pattern to a structure model containing a large number of parameters in these complex materials and therefore, results may not be very reliable for single epitaxial films, which usually show a reduced number of diffraction peaks. In the case of ultrathin films the x-ray diffraction pattern gets more and more featureless when thickness is reduced, and structure refinement becomes meaningless. An alternative approach towards the study of this problem consists of an analysis of ultrathin superconducting films in superlattice structures. Superlattice configurations provide a sensitive source of quantitative structural information through the refinement of x-ray diffraction spectra. Complementary, transmission electron microscopy (TEM) supplies real space measurements of the microstructure with a spatial resolution about a few angstroms. Thus we have a structural probe to study the atomic structure of defects and their distribution at short lateral scales which complements the averaged structural data provided by XRD.

In a recent Letter, we have reported on epitaxially strained $YBa_2Cu_3O_{7-\delta}$ (YBCO) layers in $YBa_2Cu_3O_{7-\delta}/PrBa_2Cu_3O_7$ (YBCO/PBCO) superlattices.[7] Since in plane YBCO lattice parameters are about 1% smaller than those of PBCO, then YBCO layers sandwiched between PBCO show significant epitaxial strain. In this work, apart of presenting additional XRD data complementing the previous report,[7] we report complementary transmission electron microscopy observations, we have examined the appearence of step disorder for sample thickness above the critical value, and discussed the effect of epitaxial strain on doping. We analyze the structure of ultrathin layers with thickness decreasing from a hundred angstroms to one unit cell. Although the thickness dependence of T_c for very thin layers has been widely discussed in recent past,[8] the issue of the superconductivity of a single unit cell has been long debated and remains an open question.[9,10] Our study indicates that epitaxial strain for YBCO thickness below 4 unit cells, causes important changes in interatomic distances. We propose that these structural modifications may be partly responsible for the changes in the critical temperature. The possibility of overdoping of the CuO_2 planes as a consequence of structural rearrangements is examined, although deoxygenation of epitaxially strained superlattices rules out this chance. While samples with thickness below the critical value (4 unit cells) show no step disorder, pointing to a 2D growth mechanism, structure relaxation for thicker layers results in the appearance of step disorder. This probably triggers a change of the growth mechanism into 3D. Transmission electron microscopy (TEM) observations are also reported to look at the local nature of defects.

II. EXPERIMENTAL

The samples for this study were epitaxial YBCO/PBCO superlattices grown on (100) $SrTiO_3$ (STO) substrates using a high pressure (3.4 mbar pure oxygen) multitarget sputtering system. High pressure oxygen atmosphere yields a very thermalized growth at a very slow rate, 0.13 Å/s for YBCO, which allows an accurate control of film thickness. Substrate temperature was held at 900 °C. The thickness of the PBCO layer was fixed at 5 unit cells (~60 Å) while the thickness of YBCO layers was changed from 1 to 12 unit cells. The $YBCO_N/PBCO_5$ motive was repeated up to a total thickness of 1000 Å. The growth began always with PBCO layer, provided PBCO shows a smaller lattice mismatch to STO (about 0.5% in a and 1% in b) than YBCO. High angle XRD spectra were analyzed using the SUPREX 9.0 refinement program,[11] which allows obtaining not only fractional unit cell positions of the different elements in the c direction, but also disorder related parameters such as step disorder, interdiffusion, interface strain, etc. Cross section specimens for transmission electron microscopy were prepared by mechanical grinding, dimpling and argon ion milling with an acceleration voltage of 5 kV and an incidence angle of 8°. HREM studies were carried out in a JEOL 4000 EX microscope, operated at 400 kV and in a Philips CM200 field emission analytical electron microscope operated at 200 kV and equipped with a double tilt beryllium holder.

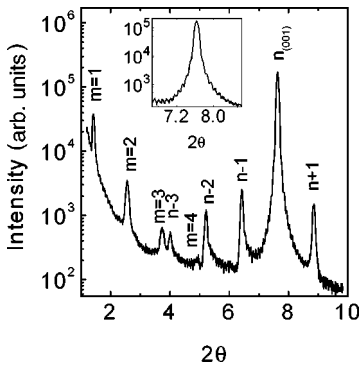

FIG. 1. Low angle x-ray diffraction pattern of a $[YBCO_1/PBCO_5]_{1000\ Å}$ superlattice. Finite size oscillations corresponding to the total thickness can be observed, pointing to a very flat surface. The well defined low angle superlattice peaks indicate a high structural perfection of the superlattice. Low angle superlattice peaks are indexed as *m*, and the satellite peaks around the (001) Bragg peaks are indexed as *n*.

III. RESULTS AND DISCUSSION

While a structural analysis of single epitaxial films by XRD is limited to obtaining lattice parameters along the growth direction, artificial superlattices are very adequate systems to study the structural implications of strained growth for two central reasons. First, a modulated structural strain profile can be obtained varying the relative thicknesses of the components. And second, the structural modulation introduced by the artificial periodicity results in a feature rich XRD pattern, which makes a spectrum refinement reliable.

Figure 1 shows a low angle diffraction spectrum for a $[YBCO_1/PBCO_5]_{1000\ Å}$ sample. Low angle spectra are sensitive to the chemical modulation of the layers through the change of the refraction index from layer to layer. Finite size oscillations can be observed below and around the first Bragg peak (inset) corresponding to a total thickness of 1000 Å. This is an indication of a surface planitude of the order of one unit cell.[12] Sharp satellite peaks from the superlattice modulation are observed, denoting very flat interfaces between YBCO and PBCO layers. Rocking curves around the (005) peak, showing FWMH as small as 0.1–0.2°, point to a very small mosaic spread in single films and superlattices. Φ scans around the (102) reflection show a perfect in plane matching, not allowing to resolve between YBCO and PBCO lattice parameters.

High angle spectra are shown in Fig. 2 with the corresponding fits for $[YBCO_N/PBCO_5]_{1000\ Å}$ samples with $N=1$ [Fig. 2(a)] and $N=8$ u.c. [Fig. 2(b)]. The refinement curve, displaced vertically for clarity, shows an excellent fit to data. The confidence factor of the fit, χ^2, was highly sensitive to the values of the fitting parameters, and was tested to sit at a meaningful mimimum for their final value. To exclude local minima in the multidimensional space of solutions the sensitivity of χ^2 to different intracell distances was checked (see Fig. 3). This was done by manually displacing single parameters from the final value in both directions, monitoring the increase in χ^2. Negligible small interdiffusion was found at the interfaces ($<5\%$ in the first layer). Random step disorder was negligible for samples with

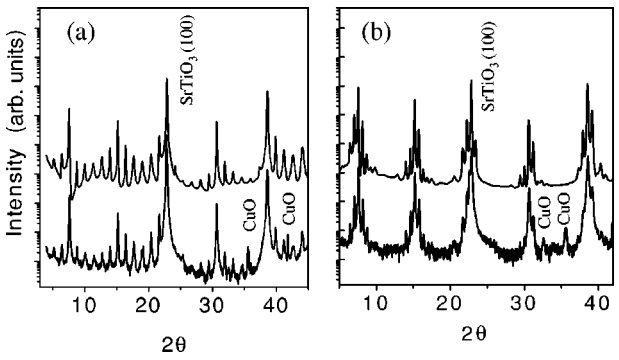

FIG. 2. XRD spectra for (a) $[YBCO_1/PBCO_5]_{1000\ Å}$ and (b) $[YBCO_8/PBCO_5]_{1000\ Å}$ superlattices together with their fits, displaced two decades vertically for clarity. Extra peaks due to CuO precipitates present in the sample are marked for clarity, together with the (100) substrate peak.

YBCO layer thickness below 3 unit cells, and was found to show up for thicker layers.

For the thinnest YBCO layers interface mismatch strain may play a major role in determining the structural details. We found a systematic and monotonous increase of the *c* parameter when YBCO layer thickness increases from 1 to 12 unit cells, approaching the value reported for single 1000 Å thick films (see Fig. 4). PBCO lattice parameter, however, remained practically unchanged. In plane PBCO lattice parameters are larger than those of YBCO by about 1%. Therefore, thin YBCO layers sandwiched in between may show in plane expansion and eventually out of plane compression. In plane expansion of YBCO due to lattice mismatch for layer thickness below four unit cells has been recently established in $YBa_2Cu_3O_{7-\delta}$.[13] Increasing YBCO thickness would relax epitaxial stress when the critical thickness, 3 or 4 unit cells from Fig. 4, is exceeded and YBCO would tend to recover single film lattice parameters (dotted line in the figure are lattice parameters of typical 1000 Å thick films).

Figure 5 shows resistance curves for representative $[YBCO_n/PBCO_5]_{1000\ Å}$ superlattices with $n=1$, 2, 4 and 8 unit cells. Sharp superconducting transitions can be seen in all cases. The critical temperature T_c was determined using the zero resistance criterion. It was also measured by ac susceptibility and values agreed within 2 K. It is widely accepted that coupling through PBCO layers, and proximity effects, enhance superconductivity in superlattices. In order to check the effect of coupling through PBCO, we measured the critical temperatures of a set of $[YBCO_1/PBCO_n]_{1000\ Å}$ samples, with PBCO thickness increasing from 1 to 20 unit cells. Samples were superconducting with a critical temperature depending on the thickness of the PBCO spacer as shown *in the inset* of Fig. 5. It can be observed that above 4 PBCO unit cells T_c becomes independent of the spacer thickness, as reported previously.[14] For the samples of this study we held PBCO layer thickness in 60 Å, approximately 5 unit cells, so, as discussed later, we can discard coupling effects as a source of T_c variations when changing YBCO layer thickness. The T_c of $[YBCO_N/PBCO_5]_{1000\ Å}$ superlattices decreases with the number of YBCO unit cells as depicted in Fig. 4. T_c values agree with previously reported data on similar superlattices.[15,16]

Additionally, interdiffusion could also be invoked to account for the depression of the critical tmperature when the YBCO thickness is reduced. It is well known that that a 45% (atomic) Pr interdiffusion into the first YBCO layer, would result in a T_c of 30 K for the resulting alloy.[15] Intriguingly,

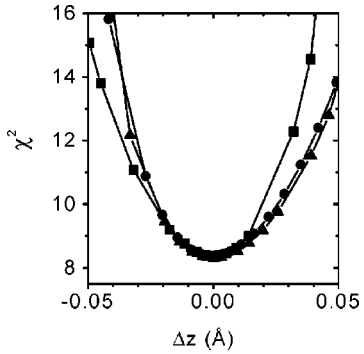

FIG. 3. χ^2 sensitivity to main intracell YBCO distances along *c* direction [squares: Y-Cu(2) distance; circles: Cu(2)-Ba distance; triangles: Ba-Cu(1) distance]. A common minimum is obtained when varying manually one of them, keeping the rest fixed in their respective final values.

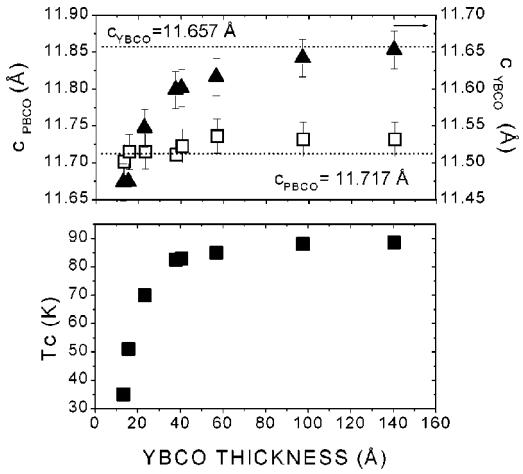

FIG. 4. Dependence of T_c and *c* parameters on YBCO layer thickness, being PBCO thickness fixed in 60 Å (5 unit cells). Dotted lines represent the typical 1000 Å thin film values.

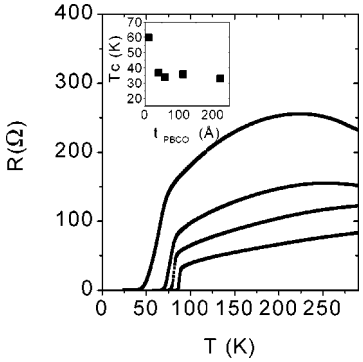

FIG. 5. Resistance curves of $[YBCO_n/PBCO_5]_{1000\ Å}$ superlattices with $n=1,2,4$, and 8 (from bottom to top). Inset: T_c values for $[YBCO_1/PBCO_m]_{1000\ Å}$ samples with *m* (PBCO spacer) ranging from 1 to 20 unit cells. Coupling through PBCO is found to saturate for PBCO layer thickness over 3 unit cells.

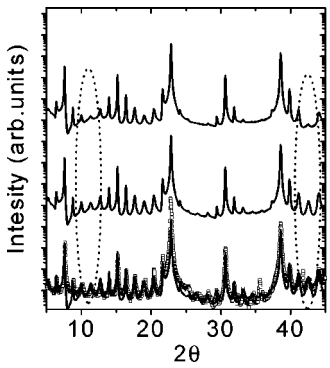

FIG. 6. Simulated XRD patterns of $[YBCO_1/PBCO_5]_{1000\ Å}$ superlattices with 0, 10, and 20 (from bottom to top) atomic percent interdiffusion of PBCO into the YBCO layer. Dots are experimental data. The depression of the intensity of high order satellites is outlined (dotted ellipses).

this value is very similar to the one obtained for the $[YBCO_1/PBCO_5]_{1000\ Å}$ superlattices. Our samples, however, showed negligible interdiffusion, less than 5% in the first layer. The SUPREX software is sensitive to interdiffusion, which is accounted for taking a weighted average of the scattering powers of the constituent materials.[11,15] Simulations of the effect of increasing such chemical disorder up to 25% in the first layer are depicted in Fig. 6, showing how the intensity of high order satellites is substantially depressed. Thus, interdiffusion should be discarded as a source for T_c reduction in our ultrathin superconducting layers.

From the observation of Fig. 4, the changes in T_c seem to correlate with those of the *c* lattice parameter, and it may be then tempting to explain the effect of epitaxial stress in terms of the results of hydrostatic pressure or uniaxial strain experiments. It is well known that YBCO shows an anomalously low T_c dependence under pressure, probably owing to the opposite dependencies on uniaxial stress in *a* and *b* directions in plane, $dT_c/d\epsilon_a = +212$ K and $dT_c/d\epsilon_b = -244$ K.[17] We can use these uniaxial strain dependencies of T_c to estimate roughly the T_c changes expected from the observed strains in YBCO/PBCO superlattices. Assuming that the structural changes for the one unit cell YBCO superlattice would occur as a result of an in plane expansion $\epsilon_a = 0.007$ and $\epsilon_b = 0.011$ due to matching with PBCO, the expected decrease of T_c would be of 1.2 K. Concerning the 1.42% decrease in the *c* lattice parameter, since $dT_c/d\epsilon_c = -8$ K, a very small increase is expected on the base of uniaxial strains. It is clear, therefore, that the superposition of the equivalent uniaxial strains of the lattice parameters due to epitaxial stress can be ruled out as a possible source of the changes in T_c when the YBCO thickness is reduced. However, it is worth stressing that in plane and out of plane strains have different signs, a situation impossible to achieve under hydrostatic pressure. Another point of interest is whether the Poisson effect holds in this system as a result of epitaxial stress. Since there are no external forces applied to the superlattice, the perpendicular components of stress σ_{cc} must vanish. The equilibrium condition should then be $\epsilon_c = -(C_{ca}\epsilon_a + C_{cb}\epsilon_b)/C_{cc}$. If both ϵ_a and ϵ_b are tensile, a compressive effect is expected in ϵ_c, according to the Poisson effect. An estimate can be done using the elastic moduli determined by Lei *et al.*[18] ($C_{ca} = 89$ GPa, $C_{cb} = 93$ GPa, and

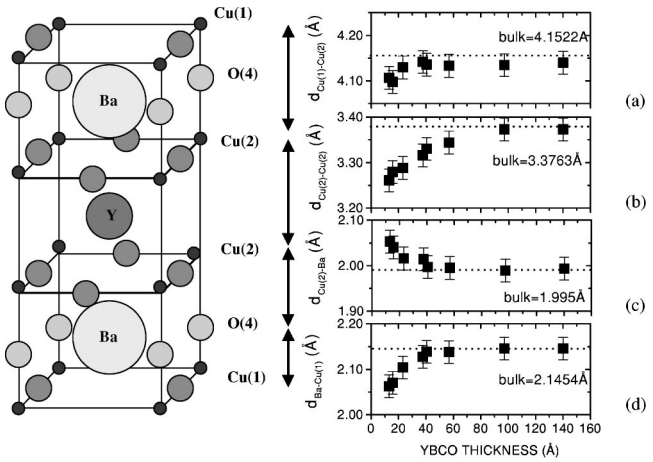

FIG. 7. Changes in the main YBCO intracell distances along the *c* axis when varying YBCO layer thickness. (a) Distance from planes to chains. (b) Distance between neighboring CuO_2 planes. (c) Plane to barium. (d) Barium to the chain. Dotted lines are the corresponding bulk values after Ref. 19.

$C_{cc} = 138$ GPa). If we again assume that for the 1 unit cell YBCO sample ϵ_a and ϵ_b are those expected from the lattice mismatch to the PBCO, a value for the *c* lattice parameter of 11.51 Å is obtained, which is close enough to the 11.49 Å obtained from the x ray fits, if one keeps in mind that films show shorter *c* lattice parameters than bulk samples. It turns out that although the Poisson effect may hold for the lattice parameters as a result of in plane lattice mismatch between YBCO and PBCO, its effect is not strong enough to account for the drastic decrease observed in T_c when the thickness of YBCO layers is reduced. We want to stress that the T_c reduction when YBCO thickness is decreased is not a superlattice effect. The same T_c, and structural results obtained for 5 PBCO cells were obtained for thicker (up to 20 unit cells) PBCO layers. Moreover, single YBCO layers sandwiched between 20 PBCO cells showed the same T_c as the superlattices, although for these samples the structure could not be refined. This means that whatever the influence of epitaxial strain within the superconducting layer is, it is the same for superlattices and single films for PBCO thickness over 5 unit cells.

However, aside from changes in the lattice parameters, the overall stress pattern gives rise to very significant and inhomogenous changes in the intracell distances, which might be responsible in their own for the changes in the superconducting properties. Figure 7 gathers the changes in some significant intracell distances in the *c* direction, like separation between consecutive CuO_2 planes, distance from the planes to the barium ion, from the barium to the chains and distance from planes to chains. Error bars describe the range over which the goodness of the fit did not significantly change, i.e., the width of the χ^2 minimum at a 3% increase. Dotted lines in the figure mark the values for the corresponding distances for bulk samples. The important new result is that epitaxial stress causes very nonhomogenous strain in the YBCO cell when the thickness of this layer is reduced up to 1 unit cell: the distance between CuO_2 planes decreases (3.8%) when the thickness is reduced and the barium approaches the chains (4%) and moves away from the planes (3%). Meanwhile, the change in the *c* lattice parameter is

only of 1.42%. When the thickness of the YBCO layer is increased intracell distances get close to bulk material values. In fact the fractional atomic positions in the unit cell in the thicker YBCO $[YBCO_8/PBCO_5]_{1000\ Å}$ and $[YBCO_{12}/PBCO_5]_{1000\ Å}$ superlattices, were in agreement within 0.5%, with those reported for bulk samples from neutron data.[2] While separation between CuO_2 planes and the distance between the barium and the chains become smaller under epitaxial stress, as qualitatively (but not quantitatively) expected from the Poisson effect, the opposite happens to the distance from the barium to the planes. It is worth remarking that, although quite large, structural changes are not unrealistic.

According to the values of the elastic moduli,[18] the 1.42% change in the *c* lattice parameter is the one expected for an uniaxial stress in the order of only 2 GPa along this direction.

Concerning the distance between consecutive CuO_2 planes which decreases by 3.8% when the YBCO thickness is reduced, it increases by a 4.9% when the rare earth is substituted from Y to Nd, increasing the ionic radius by a factor of 1.088.[19]

The distance between the CuO chains and the barium, decreasing by 4%, is also known to show a large change when oxygen content is reduced. In fact this distance increases by 5% in going from the fully oxygenated YBCO to the antiferromagnetic insulator $YBa_2Cu_3O_6$.[20]

Such changes in intracell distances may have drastic effects on the electronic structure affecting carrier concentration (doping or chain to plane charge transfer). In particular, the changes in the position of the Ba ion may modify the position of the apical oxygen affecting charge transfer. A simple reasoning in terms of electrostatic interaction would suggest that Ba atom approaching the chains may point to overdoping arising from epitaxial strain. In fact in oxygen depleted underdoped samples Ba goes away from the chains when oxygen is removed: for example, for an oxygen content $x=6.6$, the Ba atom changes its position by 2.7% approaching the planes.[2] This value is well in the range but in opposite direction to the changes observed in strained layers. In order to elucidate the possibility of overdoping we have obtained a series of deoxygenated $[YBCO_1/PBCO_5]_{1000\ Å}$ superlattices. Oxygen content was adjusted in as grown samples by *ex situ* heat treatments in controlled oxygen pressure following a stability line of the pressure temperature phase diagram. For other samples oxygen composition was adjusted in situ during sample cool down after sample growth.[21] No difference was observed between both procedures. *c* lattice parameter was found to increase when oxygen content was reduced, as usually observed in YBCO single films. Intracell distances changed upon oxygen removal, following similar trends than those reported for oxygen depleted bulk samples.[2] Annealing of the oxygen depleted samples in pure oxygen at one atmosphere and at 550 °C completely recovered the initial structure and T_c of the fully oxygenated strained superlattice, showing the reversibility and control in the process. On removing oxygen, critical temperatures were found to decrease in all cases, similarly to oxygen defficient YBCO thin films, definitely discarding overdoping as a source of T_c changes in strained ultrathin layers.

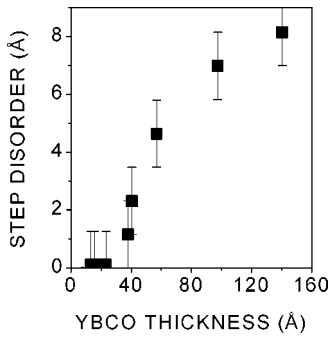

FIG. 8. Step disorder versus YBCO layer thickness. For YBCO thickness under three unit cells, step disorder is negligible. When increasing YBCO thickness over the critical one for strain relaxation (3–4 unit cells) the step disorder arises.

For YBCO layer thicknesses larger than 3 unit cells epitaxial strain is found to relax, and lattice parameters and intracell distances approximate the reported values for YBCO thicker samples (1000 Å). The release of elastic strain above the critical thickness is followed by a gradual increase in step disorder at the interfaces, probably as a result of a change in the growth mode from 2D to 3D islands. Step disorder is quantified by the SUPREX software assuming a Gaussian layer thickness fluctuation around a mean value with standard deviation σ. While σ was found to be zero for the epitaxially strained YBCO layers ($N<3$), increasing YBCO thickness above 4 unit cells resulted in an increase of the step disorder parameter, σ, up to values of 0.7 for the $N=12$ sample. Multiplying σ by the value of the *c* lattice parameter gives the mean interface roughness averaged in length scales of the order of the structural coherence length. Figure 8 shows the interface roughness dependence on YBCO layer thickness. Error bars denote the interval within the refinement does not seem to be sensitive to changes in σ. The random layer thickness fluctuation is responsible for the absence of high order satellite peaks in the XRD spectra of samples with the thicker YBCO layers, as depicted in Fig. 2.

In order to further analyze the nature of structural disorder generated by strain relaxation at a local scale, we checked the films by high resolution electron microscopy. Cross-sectional samples were studied with YBCO layer thickness changing in the desired range. Low magnification images

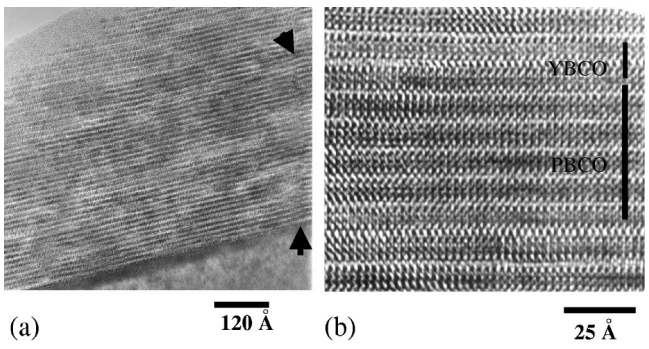

FIG. 9. (a) HREM image of a $[YBCO_1/PBCO_5]_{1000\ Å}$ sample, with the *c*-axis perpendicular to the electron beam. An antiphase boundary with a displacement of *c*/3 along the [001] direction emerging form a substrate step is marked with arrows. (b) High magnification image of the same sample.

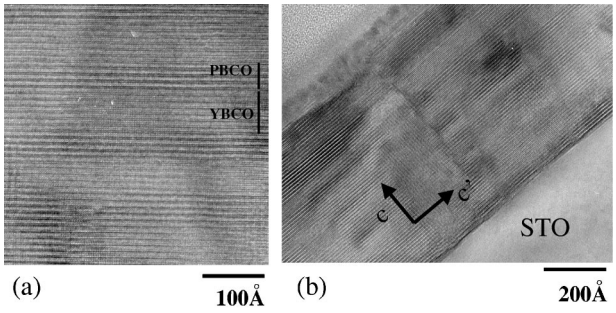

FIG. 10. (a) HREM image of a $[YBCO_8/PBCO_5]_{1000\ Å}$ sample. (b) *a*-axis oriented microdomains.

show the lateral uniformity of the layers over length scales larger than thousands of angstroms. Figures 9(a) and 9(b) show images from an epitaxially strained $[YBCO_1/PBCO_5]_{1000\ Å}$ sample. Figures 10(a) and 10(b) show images corresponding to the $[YBCO_8/PBCO_5]_{1000\ Å}$ unstrained superlattice. The latter images were taken with the sample [100] direction tilted a few degrees out of the beam direction to enhance the contrast features. Although the compositional contrast between both materials is hard to observe due to the structural similarity of YBCO and PBCO, the fluctuation in YBCO layer thickness is noticeable, confirming the presence of random step disorder for epitaxial strain released YBCO layers. Antiphase boundaries were observed in strained and relaxed samples as a result of substrate steps one unit cell high ($c/3$). Figure 9(a) shows a typical conservative antiphase boundary with a displacement of $c/3$ along the [001] direction, emerging from a substrate step and raising up to the film surface. *a*-axis oriented microdomains were found in superlattices with a relaxed structure (see Fig. 10), not showing up in the strained samples. Although this *a*-axis orientation is known to appear at substantially lower growth temperatures (600 °C), we would never expect this growth mode at our high substrate temperatures (900 °C). *a*-axis growth provides a path for a reduced lattice mismatch, and the wide distributions of these defects appearing in relaxed superlattices, might be connected to the relaxation of the epitaxial stress. In fact, the lattice mismatch between YBCO and PBCO for *c* oriented growth (0.7% and 1.1% along *a* and *b* axis, respectively), is reduced to 0.5% along the *c* direction ($c/3$) for *a*-axis growth. It is also worth noting that in this orientation, the difference between STO lattice parameter and PBCO $c/3$ length is only of 0.05%, therefore, we speculate that the apparition of *a*-axis oriented microtwins might favor a reduction of the interface energy in relaxed YBCO layers.

In summary we have shown that to some extent epitaxial stress may be complementary of pressure or cation substitution in producing internal strains affecting superconductivity. Superlattice x ray fitting of high quality $[YBCO_N/PBCO_5]_{1000\ Å}$ samples allows obtaining precise information about epitaxial strain in YBCO layers. Intracell strain increases continuously when YBCO thickness is reduced down to one unit cell. Deep nonuniform changes in some interatomic distances have been found, which seem to correlate with the decrease of T_c when thickness is reduced. In this complicated scenario it is very difficult to ascribe the changes in T_c to the changes in any particular interatomic distance. Epitaxial strain is released in layers thicker than 4 unit cells, showing lattice parameters close to those found for thicker (1000 Å) films. While no step disorder is found for the strained layers, suggesting a 2D growth mechanism, relaxed samples show a random thickness fluctuation which might be connected to a 3D growth mode. Although at present it is not possible to conclude on a direct effect on the superconductivity mechanism, epitaxial strain is a source of quite inhomogeneus changes in intracell lattice distances in ultrathin YBCO layers. Such nonuniform structural changes must be taken into account as extrinsic factors when trying to explain the decrease in the critical temperature of ultrathin YBCO films.

ACKNOWLEDGMENTS

Financial support from CICYT Grants No. MAT94-0604 and No. MAT97-0675 is acknowledged.

*On leave from Universidad del Quindio, Armenia, Colombia.

[1] A.A.R. Fernandes, J. Santamaria, S.L. Bud'ko, O. Nakamura, J. Guimpel, and I.K. Schuller, Phys. Rev. B **44**, 7601 (1991).
[2] J.D. Jorgensen, S. Pei, P. Lightfoot, D.G. Hinks, B.W. Veal, B. Dabrowski, A.P. Paulikas, and R. Kleb, Physica C **171**, 93 (1990).
[3] J.P. Attfield, A.L. Kharlanov, and J.A. McAllister, Nature (London) **394**, 157 (1998).
[4] I.K. Schuller, Nature (London) **394**, 419 (1998).
[5] J.-P. Locquet, A. Catana, E. Mächler, C. Gerber, and J.P. Bednorz, Nature (London) **394**, 453 (1998).
[6] A. Fartash, M. Grimsditch, E. Fullerton, and Y.K. Schuller, Phys. Rev. B **47**, 12 813 (1993).
[7] M. Varela, Z. Sefrioui, D. Arias, M.A. Navacerrada, M. Lucia, M.A. Lopez de la Torre, G.D. Loos, C. Leon, F. Sanchez-Quesada, and J. Santamaria, Phys. Rev. Lett. **83**, 3936 (1999).
[8] I.N. Chan, D.C. Vier, O. Nakamura, J. Hasen, J. Guimpel, S. Schultz, and Y.K. Schuller, Phys. Lett. A **175**, 241 (1993).
[9] Jakob, T. Hahn, C. Tomé-Rosa, and H. Adrian, Europhys. Lett. **19**, 135 (1992).
[10] J. Hasen, I. Lederman, and I.K. Schuller, Phys. Rev. Lett. **70**, 1731 (1993).
[11] E.E. Fullerton, I.K. Schuller, H. Vanderstraeten, and Y. Bruynseraede, Phys. Rev. B **45**, 9292 (1992).
[12] O. Nakamura, E.E. Fullerton, J. Guimpel, and I.K. Schuller, Appl. Phys. Lett. **60**, 120 (1992).
[13] J.P. Contour, M. Drouet, O. Durand, J.L. Maurice, and A. Gauzzi, Physica C **282-287**, 689 (1997).
[14] J.M. Triscone and Ø. Fischer, Rep. Prog. Phys. **60**, 1673 (1997).
[15] E.E. Fullerton, J. Guimpel, O. Nakamura, and I.K. Schuller, Phys. Rev. Lett. **69**, 2859 (1992).
[16] Q. Li, X.X. Xi, X.D. Wu, A. Inam, S. Vadlamannati, W.L. McLean, T. Venkatesan, R. Ramesh, D.M. Hwang, J.A. Martinez, and L. Nazar, Phys. Rev. Lett. **64**, 3086 (1990).
[17] W.E. Pickett, Phys. Rev. Lett. **78**, 1960 (1997) and references therein.
[18] M. Lei, J.L. Sarrao, W.M. Visscher, T.M. Bell, J.D. Thompson, A. Migliori, U.W. Welp, and B.W. Veal, Phys. Rev. B **47**, 6154 (1993).
[19] G.D. Chryssikos, E.L. Kamitsos, J.A. Kapoutsis, A.P. Patsis, V.

Psycharis, A. Koufoudakis, C. Mitros, G. Kallias, E. Gamari-Seale, and D. Niarchos, Physica C **254**, 44 (1995).

[20] R.J. Cava, A.W. Hewat, E.A. Hewat, B. Batlogg, M. Marezio, K.M. Rabe, J.J. Krajewski, W.F. Peck, Jr., and L.W. Rupp, Jr., Physica C **165**, 419 (1990).

[21] Z. Sefrioui, D. Arias, M. Varela, J.E. Villegas, M.A. López de la Torre, C. León, G.D. Loos, and J. Santamaria, Phys. Rev. B **60**, 15 423 (1999).